

# Synthesis, Characterization and Larvicidal activity of some Transition Metal Complexes of Schiff's base derived from Glutamic acid and Pyrrole-2-carboxaldehyde.

R.Subarani<sup>1</sup> and P.Metilda<sup>2\*</sup>

<sup>1</sup>Research Scholar Department of Chemistry and Research, N.M.Christian college, Marthandam, Tamilnadu-629165, India.

<sup>2\*</sup>Department of Chemistry and Research, N.M.Christian College, Marthandam, Tamilnadu-629165, India.

## Abstract:

Complexes of Cu(II), Co(II), Zn(II) and Ni(II) with a bidentate Schiff's base ligand derived from Pyrrole-2-carboxaldehyde and glutamic acid have been synthesized. The complex have been characterized by elemental analysis, IR, UV, magnetic measurement, molar conductance, NMR, ESR, TG/DTA, CV, SEM and XRD. The molar conductance measurement indicates that the above complexes are formed in 1:2 metal-ligand ratio. Based on the above studies the complexes were hexa coordinated proposing octahedral geometry. The XRD and SEM studies revealed the nano crystalline nature of the complex. The larvicidal activity of the Schiff's base and their Cu(II) complex have been also studied. The results reveal that the Cu(II) complex are showing more activity than the free ligand. Antioxidant activities of metal complexes have also been studied.

## Key words:

*Pyrrole-2-carboxaldehyde, Glutamic acid, Schiff's base, metal complexes, XRD, SEM.*

## 1. Introduction

Schiff's base complexes derived from heterocyclic compounds have increased interest in the field of bioinorganic Chemistry. The complexes derived from amino acid Schiff's bases possess anti bacterial, antifungal and antitumor activities(1-4). Transition metals are involved in many biological processes which are essential to life process. The metals can coordinate with O or N-terminals from proteins in a variety of models and play a crucial role in the conformation and function of biological macromolecules(5). Amino acid - based Schiff's bases are very effective metal chelators and their metal complexes are models for a number of important biological system(6). Recently, some researchers have reported heterocyclic Schiff's base

metal complexes derived from pyrrole-2-carboxaldehyde (7).

The present study deals with the structural aspects of some Cu(II), Co(II), Zn(II) and Ni(II) complexes with Schiff's base derived from pyrrole-2-Carboxaldehyde and Glutamic acid. The larvicidal activity of the Schiff's base and their Cu(II) complex have been also studied.

## 2. Experimental

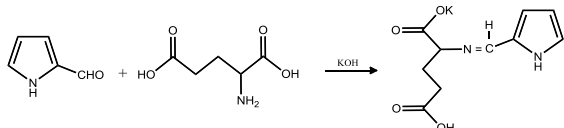
### 2.1 Material and Methods

All reagents were analytical grade producers (Aldrich) and used without further purification. Chemical analysis of Carbon, Hydrogen and Nitrogen was performed using a perkin-Elmer 2400 elemental analyzer. IR spectra of the ligand and complexes were recorded in the range of 4000-400cm<sup>-1</sup> on a shimadzu FTIR-470 Infrared spectrophotometer by KBR disc technique. UV-visible spectra was recorded using spectrophotometer with DMSO as the solvent in the range of 200-700 nm, <sup>1</sup>H NMR spectra were recorded in DMSO-d<sub>6</sub> on a Bruker Avance 111,400 MHz Spectrometer. X-ray diffraction study of some metal complexes were obtained on Bruker ASX DS Advance. Scanning Electron microscope images were recorded in JEOL model JSM -6390V electron microscopy.

### 2.2 Synthesis of Schiff's base ligand potassium(S,Z)-2-(((1H-pyrrol-2-yl)methylene)amino)-4-Carboxy butanoate.

Pyrrole-2-Carboxaldehyde (0.01mol) dissolved in 20ml MeOH is added to a methanol solution (20ml) of L-glutamic acid (0.01 mol) containing KOH (0.01

mol) in dropwise with stirring and refluxed at 60°C for 9 hours. The volume of the resulting solution was reduced to one-third. An air sensitive dark brownish yellow precipitate was filtered off washed with anhydrous ether, cold ethanol and then dried in vacuum over anhydrous CaCl<sub>2</sub>. The Schiff's base was recrystallized with ethanol and water mixture. The yield was found to be 50%.



### 2.3 Synthesis of Schiff base metal complexes:

The brownish yellow solution of Schiff's base ligand in 20ml of hot methanol (0.01 mol) a solution of metal (II) chloride in 20ml of methanol (0.005 mol) was added dropwise with constant stirring. The reaction mixture was heated for 2 hours. The precipitate was filtered off, washed several times with cold ether and then dried in vacuum over anhydrous CaCl<sub>2</sub>.

### 2.6. Antioxidant assay (Free radical scavenging activity)

The free radical scavenging activity of the Schiff base ligand PPMACB and its Cu(II), Co(II), Zn(II) and Ni(II) test samples were determined using 2,2-diphenyl-1-picrylhydrazyl(DPPH) method[8]. The different concentrations of test compound (100, 200, 400, 800 mg) and standard vitamin-C were taken in different test tubes, and volume of each test tube was adjusted to 100 µl by adding DMSO. To the sample solutions in DMSO. Methanolic solution of DPPH was added to these tubes. The tubes were allowed to stand for 15 minutes. The control experiment was carried out the same but without the any test samples. The absorbance was measured at 515 nm. Radical scavenging activity was calculated by the following formula.

$$\% \text{ Radical scavenging activity} = \left[ \frac{\text{Absorbance of Control OD} - \text{Absorbance of Sample OD}}{\text{Absorbance of control OD}} \right] \times 100$$

### 3. Results and Discussion:

The analytical data and some physical properties of the ligand and its metal complexes are noted in table 1. The data shows that the complexes are formed in the ratio 1:2 (M : L). The resulting metal complexes were found to be stable at room temperature and insoluble in common solvents such as EtOH, MeOH but soluble in DMF and DMSO.

Table: 1 Analytical data and some physical properties of the ligand and metal complexes.

Compound	Empirical Formula	Analytical data %				Molar Conductance (Ω <sup>-1</sup> cm <sup>2</sup> mol <sup>-1</sup> ) DMSO	Colour	Mel. point
		Carbon	Hydrogen	Nitrogen	Metal			
PPMACB	C <sub>10</sub> H <sub>11</sub> KN <sub>2</sub> O <sub>4</sub>	45.17(C) 45.79 (A)	4.12(C) 4.23 (A)	14.20 (C) 14.91 (A)	-	-	Brown	140
[Cu(PPMACB) <sub>2</sub> ·H <sub>2</sub> O·Cl]	C <sub>20</sub> H <sub>24</sub> CuN <sub>4</sub> O <sub>9</sub> Cl <sub>2</sub>	45.04 (C) 45 (A)	4.30 (C) 4.50 (A)	10.05 (C) 10.00 (A)	11.38 (C) 11.35 (A)	5.41	Blue	146
[Co(PPMACB) <sub>2</sub> ·H <sub>2</sub> O·Cl]	C <sub>20</sub> H <sub>24</sub> CoN <sub>4</sub> O <sub>9</sub> Cl <sub>2</sub>	45.48 (C) 45.38 (A)	4.40 (C) 4.53 (A)	10.40 (C) 10.08 (A)	10.20 (C) 10.60 (A)	15.63	Pink	185
[Zn(PPMACB) <sub>2</sub> ·H <sub>2</sub> O·Cl]	C <sub>20</sub> H <sub>24</sub> ZnN <sub>4</sub> O <sub>9</sub> Cl <sub>2</sub>	44.30 (C) 44.86 (A)	4.90 (C) 4.48 (A)	9.20(C) 9.96 (A)	11.20 (C) 11.66 (A)	19.59	Dirty White	157
[Ni(PPMACB) <sub>2</sub> ·H <sub>2</sub> O·Cl]	C <sub>20</sub> H <sub>24</sub> NiN <sub>4</sub> O <sub>9</sub> Cl <sub>2</sub>	45.10 (C) 45.40 (A)	4.70 (C) 4.54 (A)	10.50 (C) 10.08 (A)	10.10 (C) 10.56 (A)	16.78	Green	172

### 3.1 IR Spectra

The important IR spectral data of the Schiff's base ligand and its complexes are given in Table- 2. The IR spectrum of the free Schiff base ligand exhibits a sharp band at 1680 cm<sup>-1</sup> due to the azomethine group. On complexation, this band was shifted to a lower frequency in the 1643 - 1620 cm<sup>-1</sup> range indicating the coordination of the azomethine nitrogen atom to the metal ion(9). The band at 1612 and 1440 cm<sup>-1</sup> can be respectively described to asymmetric Carboxyl ν<sub>as</sub>(COO<sup>-</sup>) and symmetric Carboxyl ν<sub>s</sub>(COO<sup>-</sup>) groups. During complexation they were shifted to lower frequency by ~ 20 - 30 cm<sup>-1</sup> range indicating the linkage between the metal ion and Carboxylato oxygen atom(10). The large

difference between the ν<sub>as</sub>(COO<sup>-</sup>) and ν<sub>s</sub>(COO<sup>-</sup>) value of ~ 200 cm<sup>-1</sup> indicates the monodentate binding nature of the carboxylato group in the complexes. The IR spectra of the metal complexes also show some new bands in 525-578 and 400-486 cm<sup>-1</sup> regions which may be due to the formation of M-O and M-N bands(11). Accordingly, one can deduce that the ligand binds the metal ion as bidentate fashion. The bonding sites are the azomethine nitrogen and the carboxylato oxygen atoms. The IR spectra of Schiff's base ligand and Cu(II), Co(II), Zn(II) and Ni(II) metal complex shown in Fig. 1,2,3,4 & 5.

Table - 2 IR spectral data of the ligand and its complex( $\text{cm}^{-1}$ )

Compound	C = N	$\nu_s \text{COO}^-$	$\nu_{as} \text{COO}^-$	$\text{H}_2\text{O}$	M-O	M-N	Cl
PPMACB	1680	1440	1612	-	-	-	-
$[\text{Cu}(\text{PPMACB})_2 \cdot \text{H}_2\text{O} \cdot \text{Cl}]$	1620	1404	1525	3300	540	486	401
$[\text{Co}(\text{PPMACB})_2 \cdot \text{H}_2\text{O} \cdot \text{Cl}]$	1627	1411	1585	3062	540	400	378
$[\text{Zn}(\text{PPMACB})_2 \cdot \text{H}_2\text{O} \cdot \text{Cl}]$	1600	1411	1550	3062	525	410	393
$[\text{Ni}(\text{PPMACB})_2 \cdot \text{H}_2\text{O} \cdot \text{Cl}]$	1643	1411	1581	3350	578	400	378

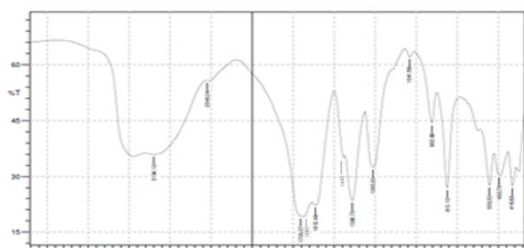
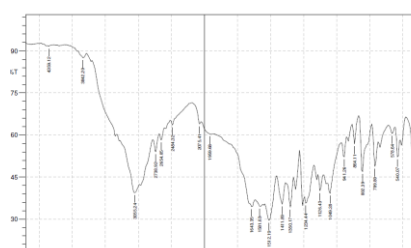
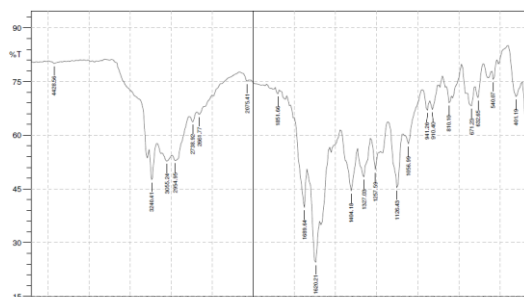
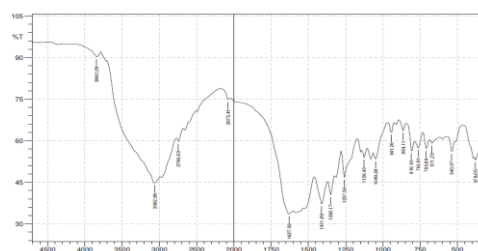
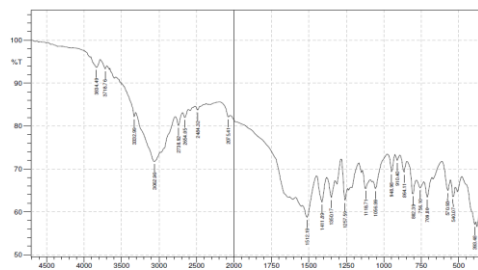


Figure 1 : IR Spectrum of the Ligand


 Fig 5:IR spectrum of  $[\text{Ni}(\text{PPMACB})_2 \cdot \text{H}_2\text{O} \cdot \text{Cl}]$ 

 Figure 2 : IR Spectrum of the  $[\text{Cu}(\text{PPMACB})_2 \cdot \text{H}_2\text{O} \cdot \text{Cl}]$ 

 Fig 3.Infrared spectrum of  $[\text{Co}(\text{PPMACB})_2 \cdot \text{H}_2\text{O} \cdot \text{Cl}]$ 

 Fig 4.Infrared spectrum of  $[\text{Zn}(\text{PPMACB})_2 \cdot \text{H}_2\text{O} \cdot \text{Cl}]$ 

### 3.2 Electronic Spectra

The electronic spectra of the complexes were recorded from freshly prepared solution of DMSO at room temperature. The electronic spectrum of Schiff's base ligand there are two absorption bands at 290, 447 nm assigned to  $\pi - \pi^*$  and  $n - \pi^*$  transitions. These transitions are also found in the spectra of the complexes, but they are shifted towards longer wavelength from ligand to complex, indicating coordination of ligand to metals through the azomethine moiety. The electronic spectrum showed the band absorption in the range 350, 490, 603 nm is assigned to  ${}^2B_{1g} \rightarrow {}^2A_{1g}$ ,  ${}^2B_{1g} \rightarrow {}^2B_{2g}$  and  ${}^2B_{1g} \rightarrow {}^2E_g$  transition. These values suggested octahedral geometry. It has been further confirmed by the magnetic moment of Cu(II) complex is 1.98 B.M corresponding to the presence of one unpaired electron and it supports an octahedral geometry(12).The Co(II) complex contains a d-d band at 743 nm, which corresponds to  ${}^4A_{2g} \rightarrow {}^4T_{1g}(P)$  transitions(13). There is a charge transfer band at 298 nm. The magnetic moment value of Co(II) complex is 4.84 B.M. The Ni(II) complex exhibits three bands at 852,433,400 nm respectively, due to the metal based transitions  ${}^3A_{2g}(F) \rightarrow {}^3T_{2g}(F)$ ,  ${}^3A_{2g}(F) \rightarrow {}^3T_{1g}(F)$ ,  ${}^3A_{2g}(F) \rightarrow {}^3T_{1g}(P)$ , indicating octahedral geometry. It has been further confirmed by the magnetic moment of Ni(II) complex is 3.12 B.M Zn(II) complexes shows only one broad band centered at 403 nm attributed to the LMCT transition which is compatible with this complex

having an octahedral structure. The Zn(II) complex is found to be diamagnetic as expected for  $d^{10}$  configuration. The UV spectrum of Schiff base

ligand and copper (II) metal complex are indicated in Figure 6 & 7.

Table 3 Electronic Spectral Data of ligand and its metal complexes

Compound	Absorption	Band assignment	Geometry and magnetic moment
PPMACB	290,447	$\pi - \pi^*$ , $n - \pi^*$	-
[Cu(PPMACB) <sub>2</sub> H <sub>2</sub> O.Cl]	294, 350, 490, 603	$\pi - \pi^*$ , ${}^2B_{1g} - {}^2A_{1g}$ , ${}^2B_{1g} \rightarrow {}^2B_{2g}$ , ${}^2B_{1g} \rightarrow {}^2E_g$	Octahedral, 1.98 BM
[Co(PPMACB) <sub>2</sub> H <sub>2</sub> O.Cl]	298, 743	$\pi - \pi^*$ , ${}^4A_{2g} \rightarrow {}^4T_1(P)$	Octahedral, 4.84BM
[Zn(PPMACB) <sub>2</sub> H <sub>2</sub> O.Cl]	259, 330, 403	$\pi - \pi^*$ , $n - \pi^*$ , LMCT	Octahedral, Diamagnetic
[Ni(PPMACB) <sub>2</sub> H <sub>2</sub> O.Cl]	400, 433, 852	${}^3A_{2g}(F) \rightarrow {}^3T_{2g}(F)$ , ${}^3A_{2g}(F) \rightarrow {}^3T_{1g}(F)$ , ${}^3A_{2g}(F) \rightarrow {}^3T_{1g}(P)$	Octahedral, 3.12 BM

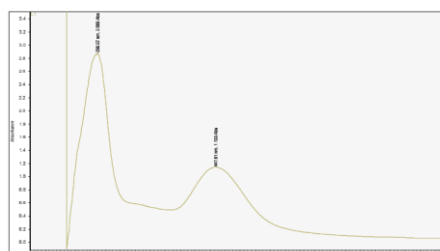


Figure 6 : UV- Visible Spectrum of the PPMACB

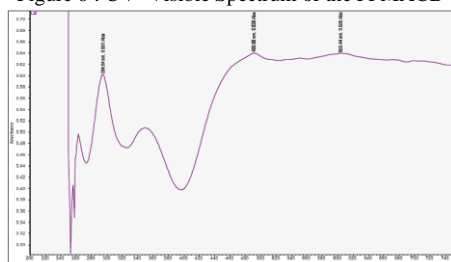


Figure 7 : UV- Visible Spectrum of the [Cu(PPMACB)<sub>2</sub>H<sub>2</sub>O.Cl]

### 3.3 <sup>1</sup>H NMR Spectra

The <sup>1</sup>H NMR spectrum of the ligand was recorded in DMSO-d<sub>6</sub>. The spectrum of the ligand showed the aromatic protons as multiplet in the range  $\delta$  6.99 - 7.01 ppm. The peaks in the region  $\delta$  6.27- 6.28 ppm were assigned to a chemical shift of pyrrole hydrogen and a singlet peak at  $\delta$  11.50 due to NH of pyrrole ring (14). The azomethine proton (HC=N) appeared as a sharp singlet at  $\delta$  8.28 ppm. Protons on the methylene group attached to a nitrogen atom, N-CH<sub>2</sub> - with resonances in the region of  $\delta$  3.40-3.90 ppm as singlet pattern. The azomethine proton of the zinc complex appeared 8.50 ppm indicating complexation of nitrogen atom of the azomethine with Zn (II). These observations suggest that the ligand coordinate to the Zn(II) through the azomethine nitrogen and carboxylate oxygen atom. In complex the peak in the region of 3.17-3.19 ppm were assigned for hydrated water and another peak at 2.5 ppm especially in DMSO solvent confirms the hydrogen bonded water molecules. A

new peak in the region 1.87-2.28 ppm characteristic of methyl group are present in the spectrum of the complex are absent in the spectrum of the ligand. The <sup>1</sup>H NMR spectrum of the ligand and Cu(II) complex is shown in Fig.8,9.

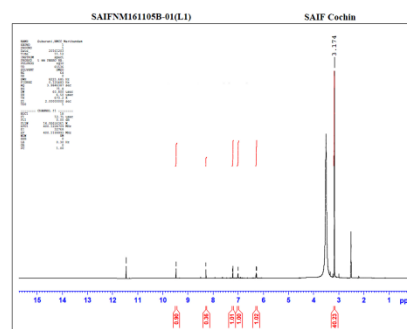


Figure 8: <sup>1</sup>H NMR spectrum of the PPMACB

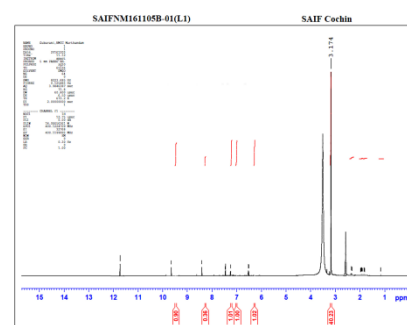


Figure 9 : <sup>1</sup>H NMR spectrum of the [Zn(PPMACB)<sub>2</sub>H<sub>2</sub>O.Cl]

### 3.4 Mass spectrum

The mass spectrum of Schiff base ligand showed of a molecular ion peak at  $m/z$  262 and it corresponds to  $[M^+]$  ion was given to Fig 10. The observed peaks are in good agreement with their empirical formula as obtained from the analytical data.

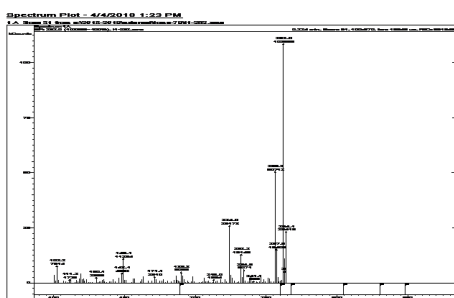
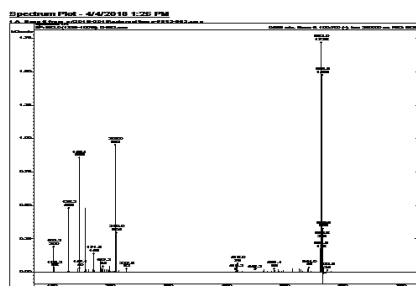


Figure 10: Mass spectrum of PPMACB

The mass spectrum of the Copper(II) complex confirms the stoichiometry of the complex. In the mass spectrum of copper(II) complex showed molecular ion peak at  $m/z = 562 [M^+]$  was given Fig11. Elemental analysis values are in close agreement with the values calculated from molecular formula assigned to these complexes. Which are further confirmed by the ESI- mass spectral study of the complexes.


 Figure 11: Mass spectrum of  $[Cu(PPMACB)_2H_2O.Cl]$ 

### 3.5 EPR spectra

The X-band EPR spectra of copper(II) complex were recorded in DMSO at liquid nitrogen temperature and at room temperature. The EPR spectra of the copper(II) complex was given fig12. The observed  $g_{||}$  and  $g_{\perp}$  values are 2.337 and 2.041 respectively. The  $g_{||}$  and  $g_{\perp}$  values are greater than 2.04, consistent with copper(II) in axial symmetry with all the principal axes aligned parallel. These  $g$  values indicate distorted octahedral stereochemistry. From the values of  $g$  factors, it is determined the geometric parameter  $G$ , representing a measure of exchange interaction between Cu(II) centres in polycrystalline compound, using the formula.

$$G = g_{||} - 2.0023 / g_{\perp} - 2.0023$$

According to Hathway (15) if  $G < 4$ , it is considered the existence of some exchange interaction between Cu(II) centres and if  $G > 4$ , the exchange interaction is negligible. The present copper complexes have  $G$  values greater than 4 indicating exchange interaction is either absent or very little in the solid complexes. The empirical ratio of  $g_{||} / A_{||}$  is frequently used to evaluate distortion in copper(II) complexes. If this ratio is close to 100, it

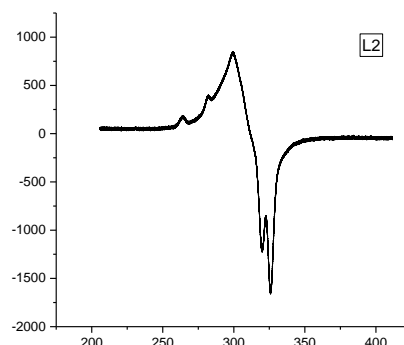
indicates roughly a square-planar structure around the copper(II) ion and the values from 170 to 250  $cm^{-1}$  are indicative of distorted tetrahedral geometry. If the ratio is in between 110 and 170, it indicates nearly an octahedral environment around copper(II) ion with small distortion. For the present copper complexes, the  $g_{||} / A_{||}$  values are 117  $cm^{-1}$  which indicate that the complex have distorted octahedral geometry.

The covalency parameters  $\alpha^2$  (covalent in-plane r-bonding) and  $\beta^2$  (covalent in-plane p-bonding) have been calculated using the following equations. If  $\alpha^2 = 1.0$ , it indicates complete ionic character where as  $\alpha^2 = 0.5$  denotes 100% covalent bonding, with assumption of negligible small values of the overlap integral.

$$\alpha^2 = (A_{||} / 0.036) + (g_{||} - 2.0027) + 3/7 (g_{\perp} - 2.0027) + 0.04$$

$$\beta^2 = (g_{||} - 2.0027) E / (-8 \lambda \alpha^2)$$

Thus, the EPR study of the copper (II) complex has to provided supportive evidence to the conclusion obtained on the basis of electronic spectrum and magnetic moment value.


 Figure 12: EPR spectrum of  $[Cu(PPMACB)_2H_2O.Cl]$ 

### 3.6 Thermo gravimetric studies.

The thermal behaviour of the copper(II) complex was examined using TG and DTA methods, in the temperature range of 40°C to 800°C at a heating rate of 10°C/min. The thermogram indicates that the complex is stable upto 200°C and then begins to decompose in three stages. Water molecules present in the complexes are of two types lattice water and coordinated water, the lattice water will be lost below 140°C and coordinated water molecules will be lost at high 140-300°C (16). In the present study Cu(II) complex decomposes in three stages, in the first stage (217°C) it shows weight loss (13%) corresponding to high temperature range this indicates that coordinated water molecules and chloride ions. In the second stage (464°C) it shows the weight loss upto (41%) and that corresponds to ligand. In the third stage (526°C) the weight loss (42%) corresponds to complete decomposition of the complex and oxidation of CuO as shown in Fig13.

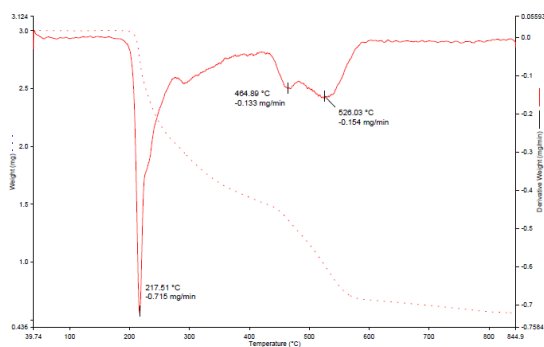


Fig 13: TG/DTA spectrum of the [Cu(PPMACB)<sub>2</sub>H<sub>2</sub>O.Cl]

### 3.7 Cyclic Voltammetry

Cyclic voltammograms were recorded in acetonitrile solution at a scan rate of 100 mV s<sup>-1</sup> in the potential range +2.0 to -2.0V. The cyclic voltammogram of the Cu(II) complex has a cathodic peak at -0.898 V versus Ag/AgCl with the corresponding anodic wave at -0.663V on the reverse scan (Fig.14). The peak separation value (ΔE<sub>p</sub> = 235 V) indicates a totally quasi-reversible character for the one-electron transfer reaction of metal based Cu(II)/Cu(I) couple.

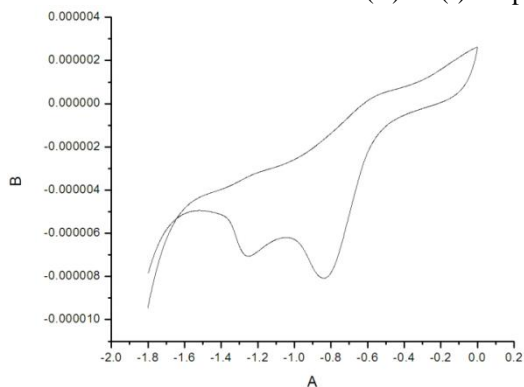


Figure 14: CV spectrum of [Cu(PPMACB)<sub>2</sub>H<sub>2</sub>O.Cl]

Based on the observations in elemental analysis, IR spectra, UV-visible spectra, <sup>1</sup>H NMR spectra, ESR, ESI-mass, TG/DTA and CV spectral studies, the proposed structure of Schiff base ligand and complexes is shown in Fig 15, 16.

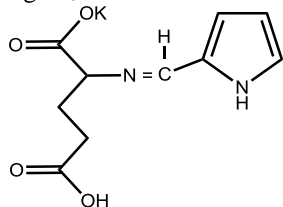


Fig 15: Structure of the ligand

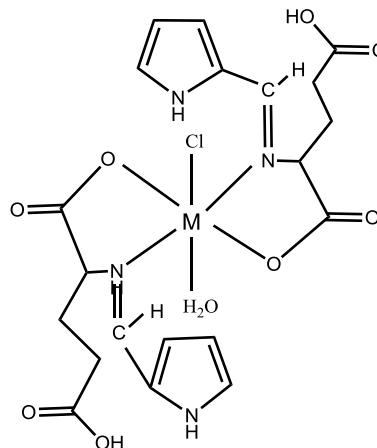


Fig 16: Structure of the Schiff base complexes of Cu(II), Co(II), Zn(II) and Ni(II) M= Cu(II), Co(II), Zn(II) and Ni(II)

### 3.8 XRD

The powder XRD patterns of Cu(II) complex were recorded over the 2θ = 0-80° range. From the data, the complexes show sharp peaks indicating their crystalline nature. The average crystalline size of the complex d<sub>XRD</sub> were calculated using Scherrer's formula (17). The Cu(II) complex has an average size of 17.79 nm, suggesting that the complex is in a nanocrystalline phase. The ligand has an average size of 26.37 nm, suggesting that the ligand is a nanocrystalline phase. The powder XRD pattern of Cu(II) complex and ligand is shown in Fig. 17 and 18.

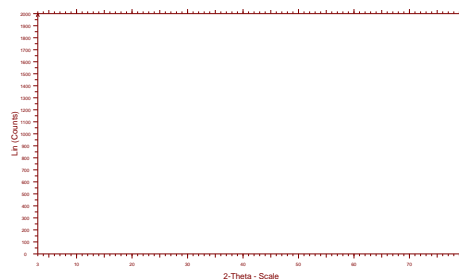


Figure 17: XRD pattern of the [Cu(PPMACB)<sub>2</sub>H<sub>2</sub>O.Cl]

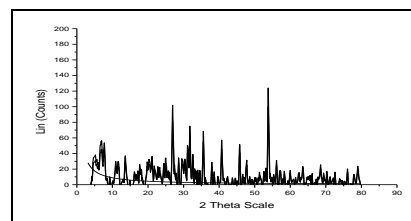


Figure 18 : XRD pattern of the PPMACB

### 3.9 SEM (Scanning Electron Microscope)

The surface morphology of the ligand is shown in Fig. 19. The SEM images of Schiff's base ligand show sharp crystalline morphology. This arrangement showed a thickness in the submicron regime. However, particles with size less than 100 nm were

also absorbed which groups to form agglomerate of larger size.

The surface morphology of Cu(II) complexes is shown in Fig.20. The SEM images of the complex has flower like morphology. The particle size is less than 100 nm which groups to form agglomerate of larger size.

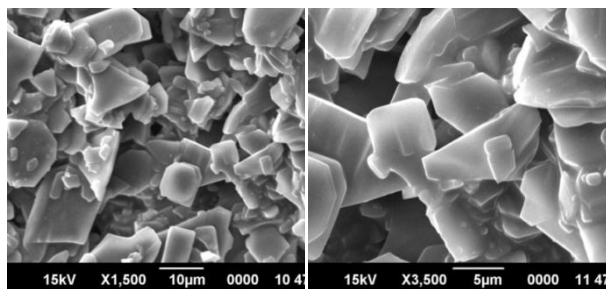


Fig 19 : SEM Photograph of the PPMACB

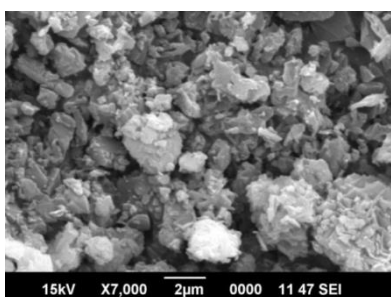


Fig 20: SEM Photograph of the [Cu(PPMACB)<sub>2</sub>·H<sub>2</sub>O·Cl]

### 3.11 EDAX Analysis

EDAX can be used to determine which chemical elements present in the sample ,and can be used to estimate their relative abundance.Elemental mapping of a sample and image analysis are also possible as showed in Fig21,22. The EDAX result of ligand showed that the atomic percentage of carbon, nitrogen, oxygen and potassium are 56.26, 8.18, 31.92 ,3.63 % respectively while that of Cu(II) complex were found to be 50.85, 45.52, 0.16, 3.47% for carbon, oxygen, chlorine and copper respectively.

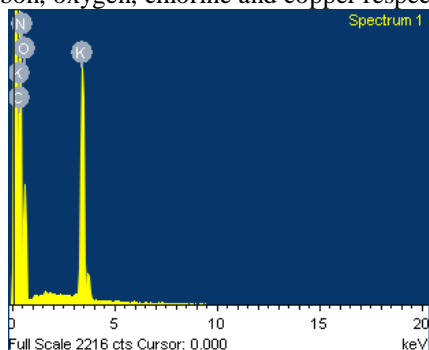


Fig21: EDAX photograph of the PPMACB

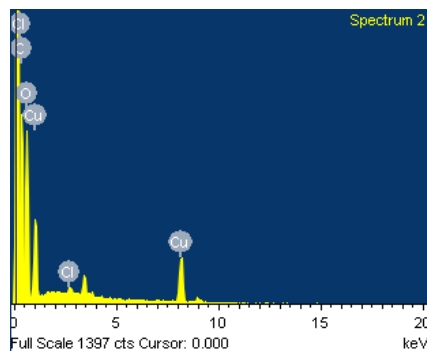


Fig 22:EDAXPhotograph of the [Cu(PPMACB)<sub>2</sub>·H<sub>2</sub>O·Cl]

### 3.12 Antioxidant activity

The synthesized Schiff base and it's metal complexes were screened for free radical Scavenging activity by the DPPH method. The results of the free radical scavenging activity of the ligand and it complexes at different concentrations are shown in Fig 23. Ni(II),Co(II) complexes have exhibited a good free radical scavenging activity. Whereas Cu(II),Zn(II), complexes have shown moderate activity. Ligand M1 showed less activity. The metal complexes were exhibited higher scavenging activity than the Schiff base ligand. The synthesized compounds scavenged the DPPH radical in a concentration dependent manner

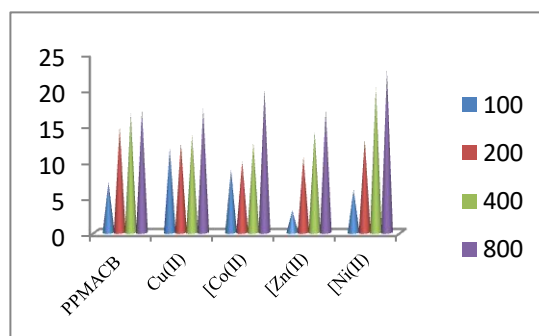


Fig 23: Antioxidant activity of Ligand and metal complexes

### 3.13 Larvicidal activity

The larvicidal activity of the Schiff base ligand and the copper complex was performed against the larvae of culex and the result of mortality values are listed in table 2,3. The pictorial representation of larvicidal activity is shown graph 3.

LC<sub>50</sub> value of copper complex = 30PPm

LC<sub>90</sub> value of copper complex = 50PPm.

LC<sub>50</sub> : Lethal concentration that kills 50 % of the exposed larvae

LC<sub>90</sub> : Lethal concentration that kills 90 % of the exposed larvae

The metal complex showed enhanced larvicidal activity than the Schiffbase. The increased mortality rate observed for cu complex can be attributed to

the increase in lipophilicity on complexation [18]. Chelation increases the lipophilic nature of the central metal atom, which in turn, favours the molecules in crossing the cell membrane of the microorganism and enhancing larvicidal activity com

Table 4 :Larvicidal activity of ligand and their Coper(II)complex

Compound	Concentration ppm	Mortality rate of different time intervals		
		24	48	72
PPMACB	1000	45	50	50
[Cu(PPMACB) <sub>2</sub> H <sub>2</sub> O.Cl]	1000	80	80	80

Table 5 : Larvicidal activity of ligand and their Coper(II) complex in various concentration

Compound	Concentration ppm	Mortality rate of different time intervals					
		12	24	36	48	60	72
[Cu(PPMACB) <sub>2</sub> H <sub>2</sub> O.Cl]	20	5	15	30	50	80	90
	40	30	85	100	100	100	100
	60	65	90	100	100	100	100
	80	75	100	100	100	100	100
	100	85	100	100	100	100	100

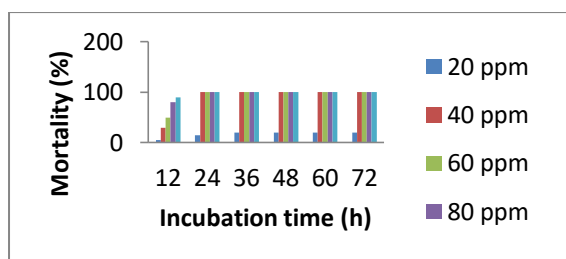


Fig24 : Larvicidal activity of Ligand and metal complexes

#### 4. Conclusion:

Schiff's base and its complexes were prepared and characterized using the elemental analysis, molar conductance, Magnetic measurement, CV, EPR, TG/DTA, SEM, EDAX, XRD, IR and electronic spectral analysis. IR spectral data shows that the ligand act as bidentate, coordinating through azomethine nitrogen and carboxylato oxygen atoms. Electronic spectral studies reveal octahedral geometry for Cu(II), Co(II), Zn(II) and Ni(II). XRD and SEM analysis explains the crystalline and morphological structure of the complexes. The larvicidal activity of the Schiff's base and their Cu(II) complex have been also studied. The results reveal that the Cu(II) complex are showing more activity than the free ligand.

#### Acknowledgement

The authors acknowledge the department of chemistry and reaserch Nesamony Memorial Christian College, Marthandam, K.K. Dist for the facilities provided, STIC, Cochin - 22 for recording the various spectra and Biogenix Trivandrum for analyzing biological activities.

#### References:

- [1] Offiong, O.E., Nfor, E., Ayi, A.A., Martelli, S., Transition Met. Chem. 25, 369. (2000).
- [2] Sakiyan, I., Glu, E.L.G., Arslan, S., Sari, N., Sakiyan, N., Biometals 17, 115. (2004).
- [3] Sari, N.E., Perihan, G., ransition Met. Chem. 28, 468.(2003).
- [4] Wang, M.Z., Meng, Z.X., Liu, B.L., Cai, G.L., Zhang, C.L., Wang, X.Y., 2005 Inorg. Chem. Commun.8, 368. (2005).
- [5] Colacio, E., Ghazi., M., Kivekas, M., Moreno, J.M., Inorg.Chem.39, 2882.(2000).
- [6] R. Karmakar, C.R. Choudhury, S. Mitra, L. Pahlenburg, Strutt. Chem., 16 1753. (2006).
- [7] Arish, D., Nair, M.S., J Coord. Chem. 63, 1619. (2010).
- [8] R.P.Singh,K.C.N.Murthy,G.K. Jaya prakasha, Agric Food.Chem. 50,81-86 (2002)
- [9] Nakamoto, K., Infrared and Raman spectra of Inorganic and Coordination compounds, fifth Ed. Wiley, New York.(1997).
- [10] Deacon, G.B., Philips, R.J., Coord. Chem.Rev. 33, 227.(1980).
- [11] El-Jouad, Riou, A., Allian, M., Khan, M.A., Bouct, G.M., Polyhedran. 20, 67. (2001).
- [12] Chandra,S.,J.Coord.chem 62,1327 (2009)
- [13] W.JGeary Coord,Chm.Rev.7.8.(1971)
- [14] Silverstain, R.M., Webster, F.X.,Spectrometric Identification of Organic Compounds.Sixth Ed. Wiley, India.(2007)
- [15] B.J. Hatha D.E..Billing Coord Chem Rev.5 141-207 (1979)
- [16] G.G.Mohamed.Spectrochimica Acta Part A: Molecular and Biomolecular Spectroscopy, 64,188(2006).
- [17] Dhanaraj, C.J., Nair, M.S, Eur. Polym. J.45, 565 (2009).